Development of a New Radioligand, *N*-(5-Fluoro-2-phenoxyphenyl)-*N*-(2-[^{18}F]fluoroethyl-5-methoxybenzyl)acetamide, for PET Imaging of Peripheral Benzodiazepine Receptor in Primate Brain

Ming-Rong Zhang,*[†,§] Jun Maeda,[‡,§] Masanao Ogawa,[†,§] Junko Noguchi,[†,§] Takehito Ito,[†,§] Yuichiro Yoshida,[†,§] Takashi Okauchi,[‡,§] Shigeru Obayashi,[‡] Tetsuya Suhara,[‡] and Kazutoshi Suzuki[†]

Department of Medical Imaging, National Institute of Radiological Sciences, 4-9-1 Anagawa, Inage-ku, Chiba 263-8555, Japan; Brain Imaging Project, National Institute of Radiological Sciences, 4-9-1 Anagawa, Inage-ku, Chiba 263-8555, Japan; and SHI Accelerator Service Co. Ltd., 5-9-11 Kitashinagawa, Shinagawa-ku, Tokyo 141-8686, Japan

Received October 1, 2003

To develop a positron emission tomography (PET) ligand for imaging the 'peripheral benzodiazepine receptor' (PBR) in brain and elucidating the relationship between PBR and brain diseases, four analogues (**4**−**7**) of *N*-(2,5-dimethoxybenzyl)-*N*-(5-fluoro-2-phenoxyphenyl)-acetamide (**2**) were synthesized and evaluated as ligands for PBR. Of these compounds, fluoromethyl (**4**) and fluoroethyl (**5**) analogues had similar or higher affinities for PBR than the parent compound **2** (K_i = 0.16 nM for PBR in rat brain sections). Iodomethyl analogue **6** displayed a moderate affinity, whereas tosyloxyethyl analogue **7** had weak affinity. Radiolabeling was performed for the fluoroalkyl analogues **4** and **5** using fluorine-18 (^{18}F, β^+; 96.7%, $T_{1/2}$ = 109.8 min). Ligands [^{18}F]**4** and [^{18}F]**5** were respectively synthesized by the alkylation of desmethyl precursor **3** with [^{18}F]fluoromethyl iodide ([^{18}F]**8**) and 2-[^{18}F]fluoroethyl bromide ([^{18}F]**9**). The distribution patterns of [^{18}F]**4** and [^{18}F]**5** in mice were consistent with the known distribution of PBR. However, compared with [^{18}F]**5**, [^{18}F]**4** displayed a high uptake in the bone of mice. The PET image of [^{18}F]**4** for monkey brain also showed significant radioactivity in the bone, suggesting that this ligand was unstable for in vivo defluorination and was not a useful PET ligand. Ligand [^{18}F]**5** displayed a high uptake in monkey brain especially in the occipital cortex, a region with richer PBR than the other regions in the brain. The radioactivity level of [^{18}F]**5** in monkey brain was 1.5 times higher than that of [^{11}C]**2**, and 6 times higher than that of (*R*)-(1-(2-chlorophenyl)-*N*-[^{11}C]methyl,*N*-(1-methylpropyl)isoquinoline ([^{11}C]**1**). Moreover, the in vivo binding of [^{18}F]**5** was significantly inhibited by PBR-selective **2** or **1**, indicating that the binding of [^{18}F]**5** in the monkey brain was mainly due to PBR. Metabolite analysis revealed that [^{18}F]**4** was rapidly metabolized by defluorination to [^{18}F]F^- in the plasma and brain of mice, whereas [^{18}F]**5** was metabolized by debenzylation to a polar product [^{18}F]**13** only in the plasma. No radioactive metabolite of [^{18}F]**5** was detected in the mouse brain. The biological data indicate that [^{18}F]**5** is a useful PET ligand for PBR and is currently used for imaging PBR in human brain.

Introduction

'Peripheral benzodiazepine receptor' (PBR), which was initially identified in the peripheral tissues, is located on the mitochondrial outer membrane in several organs including the kidney, nasal epithelium, lung, heart, and endocrine organs such as the adrenal, testis, and pituitary gland.[1−3] Later studies further demonstrated the presence of PBR in the central nervous system.[4−6] The PBR density in the brain was increased in injured brain, and this increase has been used as an indicator of neuronal damage[7] and several neurodegenerative disorders, such as Alzheimer's disease,[8] Huntington's disease,[9] Wernicke's encephalopathy,[10] multiple sclerosis,[11] and stroke.[12] In addition, a relationship between alterations of PBR and epileptic foci have been proposed.[13,14] These findings have resulted in the development of a radioligand labeled by a positron-emitter, which has made possible to visualize the distribution of PBR in the brain.[15−19]

Scheme 1. Chemical Structures of [^{11}C]**1** and [^{11}C]**2** Analogues

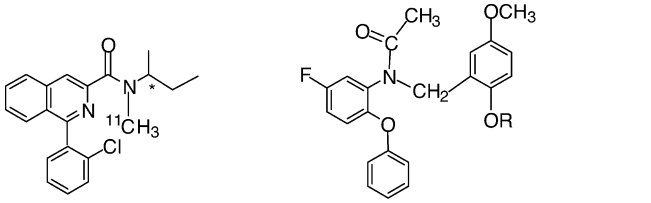

[^{11}C](*R*)-PK 11195 ([^{11}C]**1**)

DAA1106 (**2**): R = CH$_3$
[^{11}C]DAA1106 ([^{11}C]**2**): R = ^{11}CH$_3$
DAA1123 (**3**): R = H
[^{18}F]FMDAA1106 ([^{18}F]**4**): R = ^{18}FCH$_2$
[^{18}F]FEDAA1106 ([^{18}F]**5**): R = ^{18}FCH$_2$CH$_2$

(*R*)-(1-(2-Chlorophenyl)-*N*-[^{11}C]methyl,*N*-(1-methylpropyl)isoquinoline ([^{11}C](*R*)-PK 11195, [^{11}C]**1**, Scheme 1) is a clinically useful positron emission tomography (PET) ligand for imaging PBR in cases of several brain

* Corresponding author: Tel: 81-43-206-4041; Fax: 81-43-206-3261; E-mail: zhang@nirs.go.jp.
† Department of Medical Imaging, National Institute of Radiological Sciences.
‡ Brain Imaging Project, National Institute of Radiological Sciences.
§ SHI Accelerator Service Co. Ltd.

10.1021/jm0304919 CCC: $27.50
Published on Web 03/26/2004

diseases.[20−23] However, the signal of [^{11}C]**1** in the primate brain was not high enough for quantitative analysis using PET because of its low uptake into the brain.[23] Therefore, the precise characterization of PBR in primate brain awaits development of new PET ligands with improvements over [^{11}C]**1**. In 1998, *N*-(2,5-dimethoxybenzyl)-*N*-(5-fluoro-2-phenoxyphenyl)acetamide (DAA1106, **2**, Scheme 1) was reported as a potent and selective ligand for PBR by the Taisho Pharmaceutical's group.[24−27] Compound **2** had a high affinity for PBR in mitochondrial fractions of rat (K_i = 0.043 nM) and monkey (K_i = 0.188 nM) brains.[25] Moreover, **2** had weak or negligible affinities (IC_{50} > 10 μM) for other receptors, ion channels, uptake/transporters, and second messengers.[26] Thus, we previously synthesized [^{11}C]**2**[28] as a PET ligand for PBR by reacting the desmethyl precursor *N*-(5-fluoro-2-phenoxyphenyl)-*N*-(2-hydroxy-5-methoxybenzyl)acetamide[24,27] (DAA1123, **3**) with [^{11}C]-CH_3I. The in vitro and in vivo evaluation using mouse, rat and monkey demonstrated that [^{11}C]**2** had high specific binding with PBR in the brains and about a 4-fold higher uptake of radioactivity in the monkey brain than [^{11}C]**1**.[28,29] Now, [^{11}C]**2** is being used to investigate PBR in the human brain in our facility.

In general, the short half-life of a ^{11}C labeled ligand (β^+; 99.8%, $T_{1/2}$ = 20.4 min) often limits its usefulness if a dynamic PET experiment has a turnover time longer than 100 min. Since ^{18}F has advantages over ^{11}C, with a longer half-life (110 min vs. 20 min) and a lower positron energy (650 keV vs 960 keV), an ^{18}F-labeled ligand gives higher quality images with a higher spatial resolution in PET measurements. Moreover, ^{18}F is convenient for long-time storage and long-distance transportation to other facilities. To develop ^{18}F-labeled PET ligand with improved properties compared to [^{11}C]**2**, we previously prepared two [^{18}F]fluoroalkyl analogues of **2**: *N*-(5-fluoro-2-phenoxyphenyl)-*N*-(2-[^{18}F]fluoromethyl-5-methoxybenzyl)acetamide ([^{18}F]FM-DAA1106, [^{18}F]**4**) and *N*-(5-fluoro-2-phenoxyphenyl)-*N*-(2-[^{18}F]fluoroethyl-5-methoxybenzyl)acetamide ([^{18}F]-FEDAA1106, [^{18}F]**5**) as putative radioligands for PBR (Scheme 1).[30] Preliminary studies revealed that analogues **4** and **5** have similar or higher inhibitory activity (IC_{50}) for PBR in the rat brain than **2**.[30] The ex vivo autoradiograms of [^{18}F]**4** and [^{18}F]**5** binding sites in rat brain revealed significantly high radioactivity in the olfactory bulb and cerebellum, the richer regions of PBR compared with other brain regions.[30]

In this study, we synthesized four analogues (**4**−**7**, Scheme 2) including two novel compounds: (*N*-(5-fluoro-2-phenoxyphenyl)-*N*-(2-iodomethyl-5-methoxybenzyl)acetamide (**6**) and *N*-(5-fluoro-2-phenoxyphenyl)-*N*-(5-methoxy-2-tosyloxyethylbenzyl)acetamide (**7**). Using autoradiography technique, we measured the binding affinities (K_i) of **4**−**7** to PBR and the central benzodiazepine receptor (CBR). We labeled the fluoroalkyl analogues **4** and **5** using ^{18}F and prepared the radioactive products in reproducible radiochemical yields. We examined the regional distribution of [^{18}F]**4** and [^{18}F]**5** in mice and measured the percentages of unmetabolized [^{18}F]**4** and [^{18}F]**5** in the plasma and brain. Using PET, we determined the uptake of [^{18}F]**4** and [^{18}F]**5** and elucidated the specific binding of [^{18}F]**5** to PBR in the monkey brain.

Scheme 2. Chemical Synthesis of Compounds **4**−**7**[a]

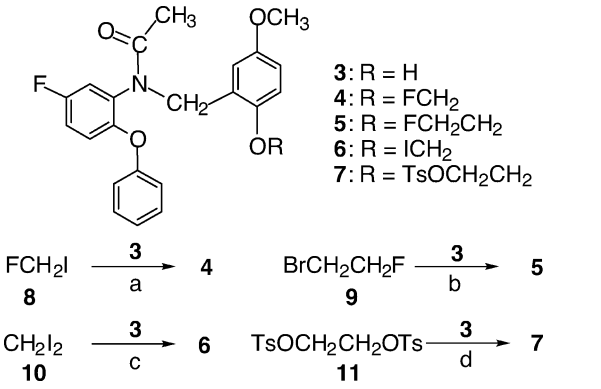

[a] Reagents and conditions: (a) NaH, DMF, 0 °C, 5 h, 79%; (b) NaH, DMF, 80 °C, 8 h, 65%; (c) NaH, DMF, 25 °C , 3 h, 34%; (d) NaH, DMF, 0 °C , 5 h, 46%.

Scheme 3. Radiosynthesis of [^{18}F]**4** and [^{18}F]**5** by Two Methods[a]

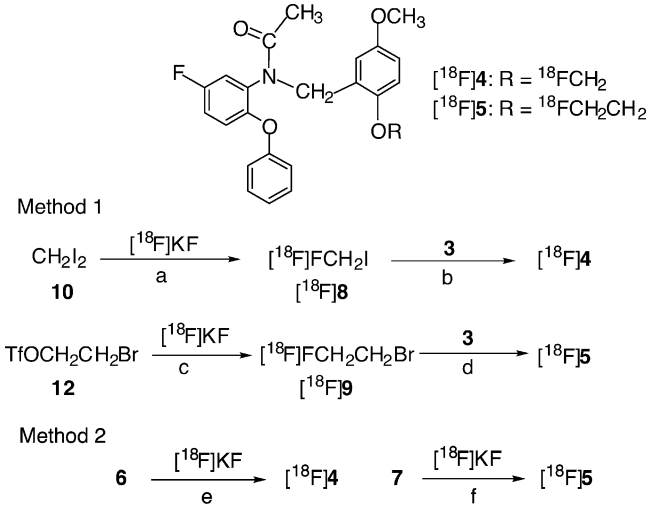

[a] Reagents and conditions: (a) 110 °C, 10 min, 8%; (b) NaH, DMF, −15 °C, 3 min, 90%; (c) *o*-dichlorobenzene, 130 °C, 5 min, 55%; (d) NaH, DMF, −15 °C, 10 min and then 120 °C, 10 min, 82%; (e) DMF, 30−120 °C, 1−15 min, 2−37%; (f) DMF, 30−120 °C, 1−15 min, 2−60%.

Results and Discussion

Chemistry. The four analogues **4**−**7** were synthesized according to the reaction sequences lineated in Scheme 2. Reaction of the desmethyl precursor **3**[24,27] with excess fluoromethyl iodide[31] (FCH_2I, **8**) in the presence of NaH at 0 °C for 5 h gave the fluoromethyl analogue **4**. Treatment of **3** with 2-fluoroethyl bromide (FCH_2CH_2Br, **9**) and NaH at 80 °C gave the fluoroethyl analogue **5**. The iodomethyl analogue **6** was prepared by the reaction of **3** with diiodomethane (CH_2I_2, **10**) and NaH at 25 °C for 3 h. The tosyloxyethyl analogue **7** was obtained by treating **3** with excess ethylene ditosylate (**11**) and NaH at 0 °C.

Radiosynthesis. Ligands [^{18}F]**4** and [^{18}F]**5** were prepared by two methods according to Scheme 3. The first method was a two-step reaction sequence which involved the preparation of the radioactive intermediate [^{18}F]fluoromethyl iodide ([^{18}F]FCH_2I, [^{18}F]**8**) or 2-[^{18}F]fluoroethyl bromide ([^{18}F]FCH_2CH_2Br, [^{18}F]**9**), followed by the alkylation of **3** with [^{18}F]**8** or [^{18}F]**9**. The second method was direct nucleophilic replacement of the iodomethyl analogue **6** or tosyloxyethyl analogue **7**

with [^{18}F]F$^-$. As for the two-step method, the alkylating intermediate [^{18}F]**8** or [^{18}F]**9** was prepared by the reaction of [^{18}F]F$^-$ with **10** or 2-trifluoromethanesulfonyloxyethyl bromide ($BrCH_2CH_2OTf$, **12**) by using a newly developed automated system.[32,33] After the fluorine reaction finished, [^{18}F]**8** or [^{18}F]**9** was purified by distillation and directly trapped in a solution of DMF containing **3** and NaH at −15 °C. The purification of [^{18}F]**8** (bp: 53−54 °C) or [^{18}F]**9** (bp: 71.5 °C) by distillation was effective, because this procedure can leave behind all nonvolatile impurities such as metal ions from the cyclotron target, the unreacted [^{18}F]F$^-$, and the phase-transfer reagent Kryptofix 222/K_2CO_3. After the radioactive [^{18}F]**8** or [^{18}F]**9** trapping ended, the [^{18}F]fluoromethylation finished perfectly, while the [^{18}F]fluoroethylation required a further 10 min at 120 °C. As for the direct method, heating **6** and **7** with [^{18}F]F$^-$ at 30−120 °C gave [^{18}F]**4** and [^{18}F]**5**. However, the radiochemical yields were not reproducible (2%−60%), and purifying [^{18}F]**4** and [^{18}F]**5** from the reaction mixtures was often difficult since the many impurities resulting from the target and reaction greatly reduced the efficiency. After comparing the reaction conditions and radiochemical yields, we synthesized [^{18}F]**4** and [^{18}F]**5** by the two-step reaction method (Method 1) via the intermediates [^{18}F]**8** and [^{18}F]**9**, respectively.

Reversed phase semipreparative HPLC purification of the reaction mixtures gave [^{18}F]**4** and [^{18}F]**5** in 45 ± 10% (n = 4) and 12 ± 4% (n = 4) radiochemical yields based on [^{18}F]F$^-$, corrected for the physical decay in a synthesis time of 63 ± 4 min and 50 ± 3 min. The identity of the desired product was confirmed by coinjection with the corresponding nonradioactive **4** or **5** on reverse phase analytic HPLC. In the final product solutions, the radiochemical purity of [^{18}F]**4** or [^{18}F]**5** was higher than 98% and the specific activity was 40−65 GBq/μmol for [^{18}F]**4** and 110−145 GBq/μmol for [^{18}F]**5** as determined from the mass measured by HPLC/UV analysis. No significant peak corresponding to **3** was observed in the HPLC for the final products. Moreover, the radiochemical purities of [^{18}F]**4** and [^{18}F]**5** remained >95% after 180 min at 25 °C, and they were stable as PET ligands while performing the evaluation.

In Vitro Binding Assays. The in vitro binding affinities (K_i) of the four analogues **4**−**7** for PBR were determined from competition for the [^{11}C]**2** binding to PBR using quantitative autoradiography of rat brain sections[34,35] (Table 1). Among these compounds, the fluoroethyl analogue **5** was the most active toward PBR. The K_i value (0.078 nM) of **5** was 2-fold higher than that of **2**, and 10-fold higher than that of **1**. This result suggested that substituting the OCH_3 group with OCH_2CH_2F group was favorable for augmenting its binding affinity for PBR. The fluoromethyl analogue **4** displayed a similar affinity to **2**, suggesting that substitution with a OCH_2F group did not obviously affect the affinity. This may be due to the molecular similarity and bioisoteric property of the OCH_2F and OCH_3 groups. The iodomethyl analogue **6** had 30 times lower affinity than **2**, while the tosyloxyethyl analogue **7** was 110 times weaker than **2**. These results suggested that the relative bulk groups in this series were not favorable for the binding of PBR. However, although it was moderately potent (K_i = 4.8 nM) for PBR, the iodomethyl analogue **6** may become a suitable candidate of a SPECT ligand for imaging PBR. Similarly, the binding affinities of **4**−**7** for CBR were measured using CBR-selective [^{11}C]flumazenil. As shown in Table 1, **4**−**7** did not display significant inhibitory effects (K_i > 1 μM) on [^{11}C]flumazenil binding in the rat brain. The negligible affinities of these analogues for CBR may be due to a difference from the typical benzodiazepine structure, which resulted in high selectivity for PBR.

Table 1. In Vitro Binding Affinity (K_i) for PBR and CBR, and Octanol/Phosphate Buffer Distribution Coefficient (log D)

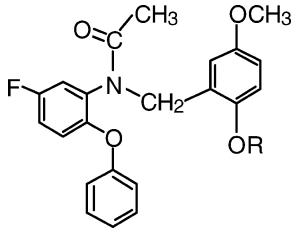

		K_i(nM)[a]		
ligand	R	PBR[b]	CBR[c]	log D[d]
4	FCH_2	0.17 ± 0.02	>1000	3.70
5	FCH_2CH_2	0.078 ± 0.01	>1000	3.81
6	ICH_2	4.8 ± 0.68	>1000	4.02
7	$TsOCH_2CH_2$	18.1 ± 1.30	>1000	4.65
2	CH_3	0.16 ± 0.02	>1000	3.65
1		0.83 ± 0.24	>1000	2.78

[a] Values represent the mean obtained from 9 concentrations of compound using at least 8 slices of rat brain (n = 3). [b] [^{11}C]**2** was incubated in the presence of the compounds examined. [c] [^{11}C]Flumazenil was incubated in the presence of the compounds examined. [d] The logD values were determined in the phosphate buffer (pH = 7.4)/octanol system using the shaking flask method. All results were presented as mean values (n = 3) with a maximum range of ±5%.

Biodistribution on Mice. The radioactivity distribution of [^{18}F]**4** and [^{18}F]**5** was measured in mice over 120 min (the data are shown in Supporting Information). These results revealed that [^{18}F]**4** and [^{18}F]**5** showed a similar distribution pattern of radioactivity in the regions examined except bone. As can be seen, high radioactivity levels (>5% ID/g) were found in tissues such as the lung, heart, kidney, and adrenal gland, organs known to be rich in PBR. The distribution patterns of uptake were in agreement with that of PBR in the peripheral system, which was consistent with the distribution of [^{11}C]**2** or [^{11}C]**1** in the mouse. The highest accumulations of [^{18}F]**4** and [^{18}F]**5** were found in the lung and these high levels were probably due to the high mitochondrial contents containing PBR in the organ. On the other hand, high radioactivities (2.6−4.4% ID/g for [^{18}F]**4** and 2.2−4.9% ID/g for [^{18}F]**5**) were also found in the brain, the target tissue in this experiment. The values were about 1.3−1.6-fold higher than that of [^{11}C]**2**, and 2−3-fold higher than that of [^{11}C]**1**, which was consistent with their higher partition coefficients as shown in Table 1. These findings suggested that [^{18}F]**4** and [^{18}F]**5** do pass across the brain−blood barrier (BBB), which is a prerequisite for a promising PET ligand.

In the bone of mouse, a significant difference in radioactivity was observed between [^{18}F]**4** and [^{18}F]**5**. The accumulation of [^{18}F]**5** in the bone was initially low and showed no increase from 30 min (0.31% dose/g) to 120 min (0.09% dose/g), which demonstrated the ex-

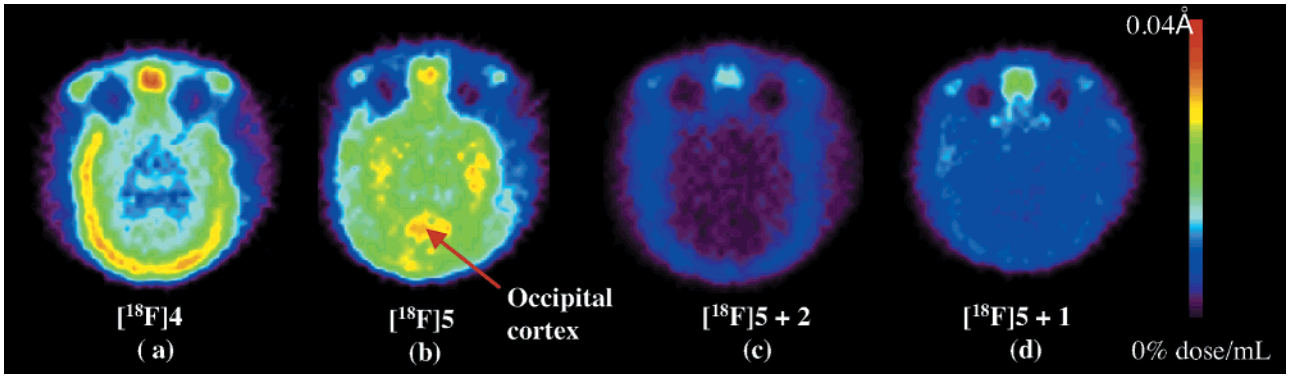

Figure 1. PET summation images of the monkey brain acquired between 30 and 180 min after [^{18}F]ligand injection. The images were obtained from the same subject. (a) [^{18}F]**4**; (b) [^{18}F]**5**; (c) [^{18}F]**5** after treatment with **2** (1 mg/kg); (d) [^{18}F]**5** after treatment with **1** (5 mg/kg). Significant radioactivity was observed in the bone after injection of [^{18}F]**4** (a). High radioactivity was observed in the occipital cortex after injection of [^{18}F]**5** (b), which was significantly inhibited by **2** (c) and **1** (d).

pected stability of the fluoroethyl group against in vivo defluorination. In contrast, after injection of [^{18}F]**4**, the radioactivity began to accumulate in the bone and reached 5.6% dose/g at 120 min, which was 50 times higher than that of [^{18}F]**5** in the bone. On consideration of the characteristic of [^{18}F]F^- to readily accumulate in bone, [^{18}F]**4** may be decomposed to [^{18}F]F^- by in vivo defluorination. Our previous findings also demonstrated that [^{18}F]fluoromethyl compounds are relatively unstable in comparison with the corresponding [^{18}F]fluoroethyl and [^{11}C]methyl compounds.[33] Therefore, [^{18}F]**4** may not be a useful PET ligand, even if it entered the brain and had some binding sites with PBR.

Monkey PET. The uptake of [^{18}F]**4** and [^{18}F]**5** in monkey brain was examined using PET. In the previous in vitro study for postmortem human brain, the highest density of PBR was observed in the occipital cortex,[36] so the region of interest (ROI) in this PET experiment was placed on the occipital cortex. Figure 1 shows typical PET summation images of the monkey brain acquired from 30 to 180 min after [^{18}F]**4** (a) and [^{18}F]**5** (b) injection (80−85 MBq/1.5 mL). The two images displayed a high accumulation of radioactivity in the brain especially in the occipital cortex. However, in comparison with [^{18}F]**5**, a marked accumulation of [^{18}F]**4** was observed in the bone. This image is visual evidence that [^{18}F]**4** was decomposed to [^{18}F]F^- in vivo as reflected in the high accumulation of [^{18}F]**4** in the mouse bone. Therefore, no further evaluation of [^{18}F]**4** was carried out using PET in monkey brain.

Figure 2 (circles) shows the time activity curve (TAC) of [^{18}F]**5** in the occipital cortex of monkey brain after intravenous (iv) injection. At 2 min after injection, a high level of radioactivity was observed in the occipital cortex, which then remained almost same level during PET measurement (180 min). The radioactivity of [^{18}F]**5** was 1.5 times higher than that of [^{11}C]**2**,[29] and 6 times higher than that of [^{11}C]**1**[29] at 30 min after injection. Pretreatment with nonradioactive **2** (1.0 mg/kg) gave a marked reduction of uptake for the image (Figure 1c) and TAC (Figure 2: triangles) of [^{18}F]**5** as compared to the control experiment which was obtained under the same conditions. As shown in Figure 2, pretreatment with **1** enhanced the initial maximal uptake of [^{18}F]**5**. The increase may be derived from [^{18}F]**5** dispossessed by mass nonradioactive **2** from lung abundant in PBR. Similar cases have been reported in the PET studies of

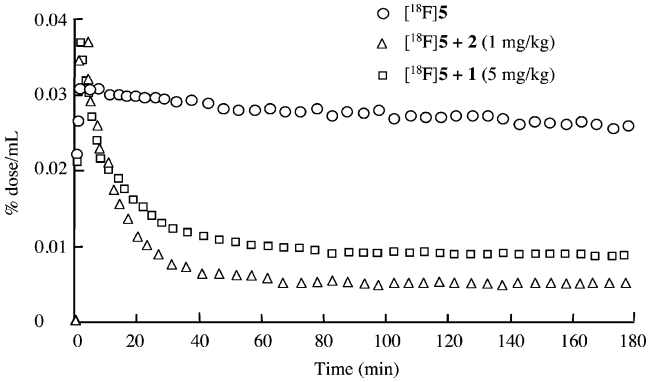

Figure 2. Time−activity curves (TACs) of [^{18}F]**5** in the occipital cortex of monkey brain. The radioactivity of the control (circles) was strongly inhibited by pretreatment with **2** (triangles) and **1** (squares).

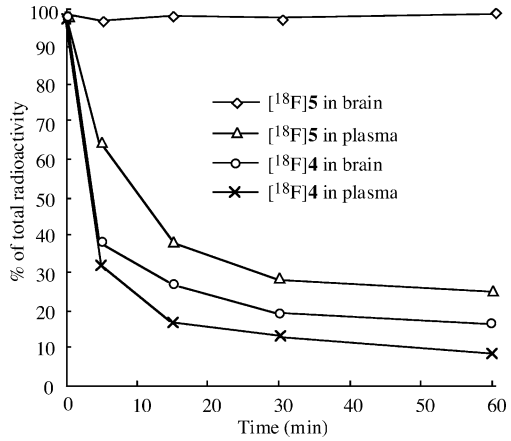

Figure 3. Percent conversion of [^{18}F]**4** or [^{18}F]**5** to metabolite in the mouse plasma and brain at several time points after iv injection of ligand (5−10 MBq) into the mice (n = 3). The unchanged tracers and metabolites were analyzed by HPLC for CH_3CN extracts from the plasma and brain homogenate prepared as described in the Experimental Section.

[^{11}C]**1**[36] and [^{11}C]**2**.[29] From 30 min after injection to the end (180 min) of the PET scan, pretreatment with **2** reduced the level of radioactivity to about 20% of the control. This result suggested high specific binding of [^{18}F]**5** present in the occipital cortex. Pretreatment with the PBR-selective **1** (5 mg/kg) also produced a significant reduction of radioactivity in the occipital cortex, as shown in the image (Figure 1d) and TAC (Figure 2: squares). The radioactivity was reduced to about 30%

Scheme 4. Metabolism of [^{18}F]**4** and [^{18}F]**5** in the Plasma and Brain

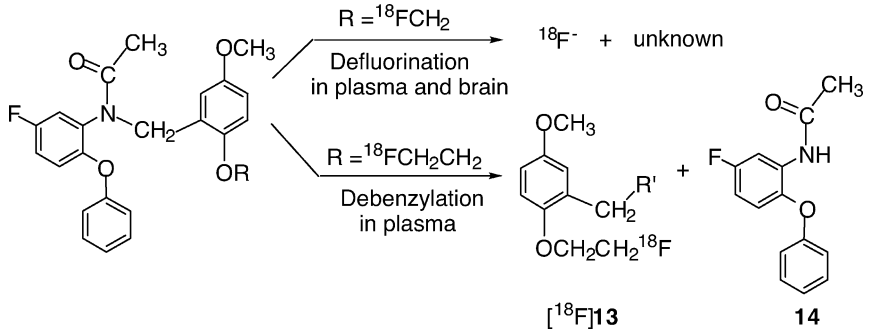

of the control from 30 min after injection to the end of the PET scan. The reduction percentage on the uptake of [^{18}F]**5** by **1** was slightly lower that by **2**, which was probably due to the weaker affinity of **1** for PBR and its lower penetration[27] into the brain than that of **2**. These findings confirmed that [^{18}F]**5** may have high specific binding for PBR in the monkey brain.

Metabolite Analysis. In the imaging brain study, the presence of metabolites in the plasma of the subject may preclude the evaluation of a PET ligand if the metabolites enter the brain and are retained/bound at the target sites. Therefore, metabolite analyses were performed for [^{18}F]**5** in the plasma and brain of mouse, and the plasma of monkey. For comparison, similar analyses were also performed for [^{18}F]**4**.

Figure 3 shows the percentages of unchanged [^{18}F]**4** and [^{18}F]**5** in the plasma and brain homogenate of mice measured by HPLC. After injection into the mouse, the fraction corresponding to the unmetabolized [^{18}F]**4** in the plasma or brain rapidly decreased to 32% or 35% at 5 min, and to 15% or 22% at 30 min. A major radioactive metabolite with high polarity was observed in the HPLC. Using ion exchange chromatography, the metabolite was assigned to [^{18}F]F$^-$. Since [^{18}F]F$^-$ is probably not brain permeable, [^{18}F]**4** may be metabolized in the plasma and brain, respectively (Scheme 4).

After its injection into the mouse, the amount of [^{18}F]**5** in the plasma continued to decrease during the entire experiment. The fraction corresponding to the unchanged [^{18}F]**5** in the plasma was 64% at 5 min, 29% at 30 min, and 25% of the total radioactivity at 60 min after injection. No [^{18}F]F$^-$ but another radioactive metabolite was observed in the HPLC. As estimated by its retention time (t_R = 1.9 min), the metabolite was much more polar than [^{18}F]**5** (t_R = 11.8 min). On the other hand, only [^{18}F]**5** was detected in the brain homogenate with no evidence (<5%) of any radioactive metabolites even at 60 min after injection.

The metabolite analysis was also performed using monkey plasma. After its injection into the monkey, [^{18}F]**5** in plasma decreased to 77% at 5 min, 56% at 30 min, and 18% at 90 min. From then, the amount of unchanged [^{18}F]**5** continued to decrease, while that of a radioactive metabolite increased to 90% by the end (180 min) of the PET experiment. The radioactive metabolite in the monkey plasma was the same metabolite determined in the mouse plasma.

As reported previously, debenzylation of **2** and [^{11}C]**2** was a main route of metabolism.[25,28] Since the fluoroethyl analogue [^{18}F]**5** had molecular similarity to and the bioisoteric property of [^{11}C]**2**, it may be metabolized with a similar profile to [^{11}C]**2** (Scheme 1). A radioactive metabolite ([^{18}F]**13**) with a benzyl moiety and nonradioactive metabolite (*N*-(5-fluoro-2-phenoxyphenyl)acetamide (**14**) may be the putative metabolite of [^{18}F]**5**. The debenzylated compound **14** had no affinity for PBR and CBR (IC_{50} > 10 μM).[25] Therefore, the presence of the nonradioactive **14** could not interfere with the specific binding of [^{18}F]**5** to PBR in the brain, even if it passed the BBB and entered the brain. Since no radioactive metabolites including [^{18}F]**13** were detected in the mouse brain homogenates, the chemical structure of [^{18}F]**13** was not further identified. These findings could reveal that although [^{18}F]**5** was extensively metabolized in the plasma, all of the specific binding determined in the monkey brain may be due to this ligand itself and not influenced by its radioactive or nonradioactive metabolite.

Conclusion

To develop PET ligands for imaging PBR in the primate brain, four analogues **4**−**7** for PBR were synthesized and evaluated in this time. The two fluoroalkyl analogues **4** and **5** had higher or same affinities for PBR than the parent compound **2** and had no potency for CBR. The iodomethyl analogue **6** had a moderate affinity for PBR and may become a candidate for a SPECT ligand. The PET ligands [^{18}F]**4** and [^{18}F]**5** were respectively synthesized by the alkylation of the desmethyl precursor **3** with [^{18}F]**8** and [^{18}F]**9** in reproducible radiochemical yields. The distribution patterns of [^{18}F]-**4** and [^{18}F]**5** in mice were consistent with the distribution of PBR. However, compared with [^{18}F]**5**, [^{18}F]**4** exhibited a high accumulation of radioactivity in the bone. The PET image of [^{18}F]**4** in the monkey brain also showed significant radioactivity in the bone, indicating that it was not a useful PET ligand because of its remarkable in vivo defluorination. The uptake of [^{18}F]**5** in the occipital cortex of the monkey brain was 1.5 times higher than that of [^{11}C]**2**, and 6 times (maximum value) higher than that of [^{11}C]**2**. Pretreatment with **1** or **2** significantly reduced the radioactivity levels of [^{18}F]**5** to 20−30% of the control in the brain, suggesting a high specific binding of [^{18}F]**5** to PBR in the monkey brain. No radioactive metabolite of [^{18}F]**5** was detected in the brain although it was metabolized in the plasma by debenzylation. This study has succeeded in developing a potential PET ligand [^{18}F]**5** which has high specific binding for PBR in the monkey brain.

Experimental Section

^{1}H NMR spectra were recorded on a JNM-GX-270 spectrometer (JEOL, Tokyo) with tetramethylsilane as an internal

standard. All chemical shifts (δ) were reported in parts per million (ppm) downfield from the standard. FAB-MS was obtained on a JEOL NMS−SX102 spectrometer (JEOL, Tokyo). Column chromatography was performed using Merck Kieselgel gel 60 F_{254} (70−230 mesh). 18-Fluorine (^{18}F) was produced by the ^{18}O (p, n) ^{18}F nuclear reaction using a CYPRIS HM-18 cyclotron (Sumitomo Heavy Industry, Tokyo). If not otherwise stated, radioactivity was determined with an IGC-3R Curiemeter (Aloka, Tokyo). HPLC was performed using a JASCO HPLC system (JASCO, Tokyo): effluent radioactivity was monitored using a NaI (Tl) scintillation detector system. Samples **2** and **3** were kindly provided by Dr A. Nakazoto (Taisho Pharmaceutical). All chemical reagents with the highest grade commercially available were purchased from Aldrich Chem. (Milwaukee, WI) and Wako Pure Chem. Ind. (Osaka). The animal experiments were carried out according to the recommendations of the committee for the care and use of laboratory animals, National Institute of Radiological Sciences (NIRS).

Chemistry. *N*-(5-Fluoro-2-phenoxyphenyl)-*N*-(2-fluoromethyl-5-methoxybenzyl)acetamide (4). A mixture of **3** (19 mg, 0.05 mmol), FCH_2I (**4**, about 20 mg in 1 mL of CH_3CN), and NaH (4 mg, 0.1 mmol) in DMF (2 mL) was stirred at 0 °C for 5 h. The reaction mixture was quenched with AcOEt and washed with water and a saturated NaCl solution. After the organic layer was dried over Na_2SO_4, the solvent was removed to give a residue. Column chromatography of the residue on silica gel with $CHCl_3$/hexane (1/9) gave **4** (16 mg, 79%) as a white powder; mp: 71−72 °C; ^1H NMR (300 MHz, $CDCl_3$) δ: 7.18−7.40 (2H, m), 6.71−7.13 (8H, m), 6.28−6.44 (1H, m), 5.30 (2H, d, J = 49 Hz), 4.80 (2H, dd, J = 2, 12 Hz), 3.71 (3H, s), 2.12 (3H, s); FABMS (m/z): 414.2 ($M^+ + 1$); Anal. ($C_{23}H_{21}F_2NO_4$) C, H, N.

***N*-(5-Fluoro-2-phenoxyphenyl)-*N*-(2-fluoroethyl-5-methoxybenzyl)acetamide (5).** A mixture of **3** (38 mg, 0.1 mmol), FCH_2CH_2Br (**9**, 25 μL, 0.2 mmol) and NaH (8 mg, 0.2 mmol) in DMF (5 mL) was heated at 80 °C for 8 h. The reaction mixture was quenched with AcOEt, and washed with water and a saturated NaCl solution. After the organic layer was dried over Na_2SO_4, the solvent was removed to give a residue. Column chromatography of the residue on silica gel with $CHCl_3$/hexane (1/13) gave **5** (27 mg, 65%) as a white powder; mp: 54−56 °C; ^1H NMR (300 MHz, $CDCl_3$) δ: 7.26−7.59 (2H, m), 6.22−7.19 (9H, m), 4.88 (2H, dt, J = 4, 41 Hz), 4.65 (2H, dd, J = 2, 12 Hz), 4.12 (2H, dt, J = 4, 27 Hz), 3.80 (3H, s), 2.15 (3H, s); FABMS (m/z): 428.2 ($M^+ + 1$); Anal. ($C_{24}H_{23}F_2NO_4$) C, H, N.

***N*-(5-Fluoro-2-phenoxyphenyl)-*N*-(2-iodomethyl-5-methoxybenzyl)acetamide (6).** A mixture of **3** (19 mg, 0.05 mmol) and CH_2I_2 (**10**, 11 μL, 0.15 mmol) in DMF (5 mL) was stirred at 25 °C for 3 h. The reaction mixture was quenched with AcOEt and washed with water and a saturated NaCl solution. After the organic layer was dried over Na_2SO_4, the solvent was removed to give a residue. Column chromatography of the residue on silica gel with $CHCl_3$/hexane (1/15) gave **6** (8.9 mg, 34%) as a colorless oil; ^1H NMR (300 MHz, $CDCl_3$) δ: 7.18−7.40 (2H, m), 6.15−7.33 (9H, m), 4.81 (dd, J = 2, 12 Hz), 4.70 (2H, s), 3.78 (3H, s), 2.20 (3H, s); FABMS (m/z): 524.1 ($M^+ + 1$); Anal. ($C_{23}H_{21}FINO_4$) C, H, N.

***N*-(5-Fluoro-2-phenoxyphenyl)-*N*-(5-methoxy-2-tosyloxyethylbenzyl)acetamide (7).** A mixture of **3** (19 mg, 0.05 mmol), $TsOCH_2CH_2OTs$ (**11**, 37 mg, 0.1 mmol) and NaH (8 mg, 0.2 mmol) in DMF (5 mL) was stirred at 0 °C for 5 h. The reaction mixture was quenched with AcOEt and washed with water and a saturated NaCl solution. After the organic layer was dried over Na_2SO_4, the solvent was removed to give a residue. Column chromatography of the residue on silica gel with $CHCl_3$/hexane (1/20) gave **7** (14 mg, 46%) as a colorless oil; ^1H NMR (300 MHz, $CDCl_3$) δ: 6.52−7.48 (15H, m), 4.62 (2H, dd, J = 2, 12 Hz), 4.43−4.28 (2H, m), 4.12−3.92 (2H, m), 3.80 (3H, s), 3.36 (3H, s), 2.32 (3H, s); FABMS (m/z): 580.3 ($M^+ + 1$); Anal. ($C_{31}H_{30}FNSO_7$) C, H, N.

Radiosynthesis. [^{18}F]Fluoride ([^{18}F]F^-). [^{18}F]F^- was produced by the ^{18}O (p, n) ^{18}F reaction on 10−20 at. % $H_2{}^{18}O$ using 18 MeV protons (14.2 MeV on target) from the cyclotron and separated from [^{18}O]H_2O using Dowex 1-X8 anion-exchange resin in an irradiating room. The [^{18}F]F^- was eluted from the resin with aqueous K_2CO_3 (3.3 mg/0.3 mL) into a vial containing CH_3CN (1.5 mL)/4,7,13,16,21,24-hexaoxa-1,10-diazabicyclo[8,8,8]hexacosane (Kryptofix 222, 25 mg) and transferred into a reaction vessel in a hot cell.

***N*-(5-Fluoro-2-phenoxyphenyl)-*N*-(2-[^{18}F]fluoromethyl-5-methoxybenzyl)acetamide ([^{18}F]4).** [^{18}F]F^- from the irradiating room was transported to a Pyrex glass vessel (5 mL) containing 100 μL of *o*-dichlorobenzene (*o*-DCB), and the [^{18}F]F^- was dried to remove H_2O and CH_3CN at 120 °C for 15 min. After CH_2I_2 (**10**, 100 μL) was added to the radioactive mixture by a helium flow (50 mL/min) at 120 °C, [^{18}F]FCH_2I ([^{18}F]**8**) resulted in this vessel was distilled at once under helium for 3 min and bubbled into another Pyrex glass vessel containing the demethyl precursor (**3**, 1.5 mg) and NaH (10 μL, 1.5 g/20 mL DMF) in anhydrous DMF (300 μL) at −15 °C. After maximum radioactivity was bubbled into the solution, the reaction was terminated by adding CH_3CN/H_2O (6/4, 500 μL). The radioactive mixture was applied to a semipreparative HPLC column. HPLC semipreparative purification was completed on YMC J'sphere ODS−H80 column (10 mm ID × 250 mm) using a mobile phase of CH_3CN/H_2O (60/40) at a flow rate of 6.0 mL/min. The retention time (t_R) for [^{18}F]**4** was 11.2 min, whereas that for **3** was 6.7 min. The radioactive fraction corresponding to [^{18}F]**4** was collected in a sterile flask containing polysorbate (80) (75 μL) and ethanol (150 μL), evaporated to dryness under vacuum, redissolved in 7 mL of sterile normal saline, and passed through a 0.22 μm Millipore filter to obtain the final product. At the end of synthesis (EOS), 180−300 MBq of [^{18}F]**4** was obtained as an iv injectable solution at a beam current of 10−15 μA and 20−25 min proton bombardment.

***N*-(5-Fluoro-2-phenoxyphenyl)-*N*-(2-[^{18}F]fluoroethyl-5-methoxybenzyl)acetamide ([^{18}F]5).** After the [^{18}F]F^- was dried, $BrCH_2CH_2OTf$ (**12**, 8 μL) in *o*-dichlorobenzene (400 μL) was added to the radioactive mixture. The [^{18}F]FCH_2CH_2Br ([^{18}F]**9**) in this vessel was distilled under a helium flow (90−100 mL/min) at 130 °C for 5 min and bubbled into another vessel containing **3** (1.5 mg) and NaH (10 μL, 1.5 g/20 mL DMF) in anhydrous DMF (300 μL) at −15 °C, and the reaction mixture was heated and kept at 120 °C for 10 min. HPLC semipreparative purification was performed on a YMC J'sphere ODS−H80 column (10 mm ID × 250 mm) using a mobile phase of CH_3CN/H_2O (55/45) at a flow rate of 6.0 mL/min. The t_R for [^{18}F]**5** was 14.2 min. At EOS, 570−780 MBq of [^{18}F]**5** was obtained as an iv injectable solution at a beam current of 10−15 μA and 20−25 min proton bombardment.

Radiochemical Purity and Specific Activity Determinations. Radiochemical purity was assayed by analytical HPLC (column: CAPCELL PAK C_{18}, 4.6 mm ID × 250 mm, UV at 254 nm; mobile phase: CH_3CN/H_2O = 6/4). The t_R for [^{18}F]**4** and [^{18}F]**5** was 6.1 and 6.3 min at a flow rate of 2.0 mL/min. The specific activity of [^{18}F]**4** and [^{18}F]**5** was determined by comparison of the assayed radioactivity to the mass associated with the carrier UV peak at 254 nm.

In Vitro Binding Assays. Male Sprague−Dawley rats (n = 4) weighing 220−250 g were killed by decapitation under ether anesthesia, and their brains were quickly removed and frozen on powdered dry ice. Brain sagittal sections (20 μm) were cut on a cryostat microtome (HM560, Carl Zeiss Co., Germany) and thaw-mounted on glass slides (Matsunami Glass Ind., Tokyo), which were then dried at room temperature and stored at −18 °C until use for experiments. The brain sections were preincubated at 25 °C for 20 min in 50 mM Tris-HCl (pH 7.4) buffer. After the preincubation, these sections were incubated at 37 °C for 30 min in the assay buffer containing [^{11}C]**2** (1 nM, specific activity: 110 GBq/μmol) or [^{11}C]flumazenil (1 nM, specific activity: 220 GBq/μmol). To determine the IC_{50} values of **1**, **2**, **4**−**7** for the [^{11}C]**2** (for PBR) or [^{11}C]flumazenil (for CBR) binding, the brain sections were incubated with [^{11}C]**2** or [^{11}C]flumazenil in the presence of increasing concentrations of the corresponding **1**, **2**, **4**−**7** (0.1−1000 nM). Nonradioactive **2** or flumazenil (10 μM) of was used

to determine the nonspecific binding for PBR or CBR. After the incubation, the sections were washed three times for 2 min each time with the cold assay buffer, dipped into cold distilled water, and dried with a stream of warm air (about 50 °C). These sections were then placed in contact with imaging plates (BAS−SR 127, Fuji Photo Film Co. Ltd., Tokyo, Japan) for 60 min to analyze the distribution of their radioactivity with a FUJIX BAS 3000 bioimaging analyzer (Fuji). The region of interest (ROI) on the sections was placed on the cerebellum. PSL data corresponding to the radioactivity on the cerebellum in the presence and absence of the displacement **1**, **2**, **4**−**7** were determined. Specific binding for PBR or CBR was defined as total binding minus binding in the presence of **2** or flumazenil (10 μM). The PSL data corresponding to the specific binding at each compound concentration was calculated as a percentage in relation to the control specific binding, and which were converted to probit values to determine the IC_{50} of each compound. The IC_{50} value was further converted to K_i according to the Cheng−Prusoff equation.[36]

Biodistribution on Mice. A saline solution of ^{18}F-ligand (average of 8 MBq/200 μL) was injected into ddy mice (30−40 g, 9 weeks, male) through the tail vein. Four mice for each time point were sacrificed by cervical dislocation at 5, 15, 30, 60 and 120 min after injection. Whole brain, liver, lung, heart, kidney, adrenal, bone, and blood samples were quickly removed and weighed. The radioactivity present in the various tissues was measured in a Packard autogamma scintillation counter and expressed as a percentage of the injected dose per gram of wet tissue (% ID/g). All radioactivity measurements were corrected for decay.

PET on Monkeys. The PET scan was performed using a high-resolution SHR-7700 PET camera (Hamamatsu Photonics, Hamamatsu, Japan) designed for laboratory animals, which provides 31 transaxial slices 3.6 mm (center-to-center) apart and a 33.1 cm field of view. A male rhesus monkey (*macaca mulatta*) weighing about 5 kg was repeatedly anesthetized with ketamine (Ketalar, 10 mg/kg/h, im) every hour through the session. After transmission scans for attenuation correction were performed for 1 h using a 74 MBq ^{68}Ge-^{68}Ga source. A dynamic emission scan in the 3D acquisition mode was performed for 90 min (2 min × 5 scans, 4 min × 10 scans, 10 min × 4 scans). All emission scan images were reconstructed with a Colsher filter of 4 mm, and circular regions of interest (ROIs) with a 5-mm diameter were placed over the occipital cortex using an image analysis software.[35,36] A solution of [^{18}F]**4** and [^{18}F]**5** (80−85 MBq) was injected iv into the monkey, and time-sequential tomographic scanning was performed on a transverse section of the brain for 180 min. In pretreatment experiments, nonradioactive **2** (1 mg/kg) or **1** (5 mg/kg) was injected at 2 min before the [^{18}F]**5** injection. The time activity curves (TACs) in the occipital cortex were obtained for each scan of the brain.

Metabolite Assay for Mouse Plasma and Brain Tissue. After iv injection of [^{18}F]**4** or [^{18}F]**5** (5−10 MBq/100 μL) into ddy mice (n = 3), these mice were sacrificed by cervical dislocation at 5, 15, 30, or 60 min. Blood (0.7−1.0 mL) and whole brain samples were removed quickly. The blood sample was centrifuged at 15 000 rpm for 1 min at 4 °C to separate plasma (250 μL), which was collected in a test tube containing CH_3CN (500 μL) and a solution of the authentic unlabeled **4** or **5** (1.1 mg/5.0 mL of CH_3CN, 10 μL). After the tube was vortexed for 15 s and centrifuged at 15 000 rpm for 2 min for deproteinization, the supernatant was collected. The extraction efficiency of radioactivity into the CH_3CN supernatant ranged from 70% to 92% of the total radioactivity in the plasma. On the other hand, the cerebellum and forebrain including the olfactory bulb were dissected from the mouse brain and homogenized together in an ice-cooled CH_3CN/H_2O (1/1, 1.0 mL) solution. The homogenate was centrifuged at 15 000 rpm for 1 min at 4 °C, and supernatant was collected. The recovery of radioactivity into the supernatant was 68−87% based on the total radioactivity in the brain homogenate.

An aliquot of the supernatant (100−500 μL) obtained from the plasma or brain homogenate was injected into the HPLC system for radioactivity and analyzed under the same conditions described above except that the mobile phase was CH_3CN/H_2O with a ratio of 1/1. The percent ratio of [^{18}F]ligand (t_R = 10.6 min for [^{18}F]**4** and 11.8 min for [^{18}F]**5**) to total radioactivity (corrected for decay) on the HPLC chromatogram was calculated as % = (peak area for [^{18}F]ligand/total radioactive peak area) × 100.

Metabolite Analysis for Monkey Plasma. After iv injection of [^{18}F]**5** (80 MBq) into the monkey, arterial blood samples (1 mL) were collected at 2, 10, 30, 60, 90, 120, and 180 min. All samples were centrifuged at 15 000 rpm for 1 min at 4 °C to separate plasma (250 μL), which was collected in a test tube containing CH_3CN (0.5 mL). The tube was vortexed for 15 s and centrifuged at 15 000 rpm for 1 min for deproteinization. The extraction efficiency of radioactivity into the CH_3CN ranged from 73% to 94% of the total radioactivity in the plasma. The radioactive fractions in these samples were determined using HPLC.

Acknowledgment. The authors are grateful to Dr A. Nakazoto (Taisho Pharmaceutical Co., Ltd.) for providing the samples (**2** and **3**) and helpful suggestions. We also thank the crew of the Cyclotron Operation Section and Radiopharmaceutical Chemistry Section of National Institute of Radiological Sciences (NIRS) for support in operation of the cyclotron and production of radioisotopes.

Supporting Information Available: Radioactivity distribution of [^{18}F]**4** and [^{18}F]**5**. This material is available free of charge via the Internet at http://pubs.acs.org.

References

(1) Braestrop, C.; R. F. Squires Specific Benzodiazepine Receptors in Rat Brain Characterized by High Affinity [^{3}H]Dizaepam Binding. *Proc. Natl. Acad. Sci. U.S.A.* **1977**, *74*, 1839−1847.
(2) Anholt, R. R. H.; DeSouza, E. B.; Oster-Granite, M. L.; Synder, S. H. Peripheral-type Benzodiazepine Receptors: Autoradiographic Localization in Whole-body Sections of Neonatal Rats. *J. Pharmacol. Exp. Ther.* **1985**, *233*, 517−526.
(3) Gavisg, M.; Katz, Y.; Bar-Ami, S.; Wizman, R. Biochemical, Physiological and Pathological Aspects of the Peripheral Benzodiazepine Receptor. *J. Neurochem.* **1992**, *58*, 1589−1602.
(4) Schoemaker, H.; Bliss, M.; Yamamura, H. I. Specific High Affinity Saturable Binding to [^{3}H]Ro5−4864 Benzodiazepine Binding Sites in Rat Cerebral Cortex. *Eur. J. Pharmacol.* **1981**, *71*, 473−475.
(5) Weissman, B. A.; Gordon, T. B.; Lawrence, I.; Steven, M. P.; Stolnick, P. Characterization of the Binding of [^{3}H]Ro 5−4864, a Convulsant Benzodiazepine, to Guinea Pig Brain. *J. Neurochem.* **1984**, *42*, 969−975.
(6) Zisterer, D. M.; Williams, D. C. Peripheral-type Benzodiazepine Receptors. *Gen. Pharmacol.* **1997**, *29*, 305−314.
(7) Benavides, J.; Fage, D.; Carter, C.; Scatton, B. Peripheral Type Benzodiazepine Binding Sites are a Sensitive Indirect Index of Neuronal Damage. *Brain Res.* **1987**, *421*, 167−172.
(8) Diorio, D.; Welner, S.; Butterworth, R.; Meaney, M.; Suranyl-Cadotte, R. Peripheral Benzodiazepine Binding Sites in Alzheimer's Disease Frontal Cortex and Temporal Cortex. *Neurobiol. Aging* **1991**, *12*, 255−258.
(9) Messmer, K.; Reynolds, G. P. Increased Peripheral Benzodiazepine Binding Sites in the Brain of Patients with Huntington's Disease. *Neurosci. Lett.* **1998**, *241*, 53−56.
(10) Deajardins, P.; Todd, K. G.; Hazell, H. A.; Butterworth, R. F. Increased "Peripheral-type" Benzodiazepine Receptor Sites and mRNA in Thalamus of Thiamine-Deficient Rats. *Neurochem. Int.* **1999**, *35*, 363−369.
(11) Banati R. B.; Newcombe, J.; Gunn, R. N.; Cagnin, A.; Turkheimer, F.; Heppner, F.; Price, G.; Wegner, F.; Giovannoni, G.; Miller, D. H.; Perkin, G. D.; Smith, T.; Hewson, A. K.; Bydder, G.; Kreutzberg, G. W.; Jones, T.; Cuzner, M. L.; Myers, R. The Peripheral Benzodiazepine Binding Site in the Brain in Multiple Sclerosis: Quantitative In Vivo Imaging of Microglia as a Measure of Disease Activity. *Brain* **2000**, *123*, 2321−2337.
(12) Raghavendra Rao, V. L.; Dogan, A.; Bowen, K. K. Dempsy, R. J. Traumatic Brain Injury Leads to Increased Expression of peripheral-type Benzodiazepine Receptors, neuronal Death, and Activation of Astrocytes and Microglia in Rat Thalamus. *Exp. Neurol.* **2000**, *161*, 102−114.

(13) Johnson, E. W.; De lanerolle, N. C.; Kim, J. H.; Sundaresan, S.; Spencer, D. D.; Mattson, R. H.; Zoghbi, S. S.; Baldwin, R. M.; Hoffer, P. B.; Seibyl, J. P. "Central" and "Peripheral" Benzodiazepine Receptors: Opposite Changes in Human Epieptogenic Tissue. *Neurology* **1992**, *42*, 811−815.

(14) Sauvageau, A.; Desjardins, P.; Lozeva, V.; Rose, C.; Hazell, A. S.; Bouthillier, A.; Butterwort, R. F. Increased Expression of "Peripheral-type" Benzodiazepine Receptors in Human Temporal Lobe Epilepsy: Implications for PET Imaging of Hippocampal Sclerosis. *Metab. Brain. Dis.* **2002**, *17*, 3−11.

(15) Camsonne, R.; Crouzel, C.; Comar, D.; Maziere, M.; Prenant, C.; Sastre, J.; Moulin, M. A.; Syrota, A. Synthesis of N-[^{11}C]-Methyl, N−(Methyl-1-propyl), (Chloro-2-phenyl)-1-isoquinoline Carboxamide-3 (PK11195): a New Ligand for Peripheral Benzodiazepine Receptors. *J. Labelled Comp. Radiopharm.* **1984**, *21*, 985−991.

(16) Hashimoto, K.; Inoue, O.; Suzuki, K.; Yamasaki, T.; Kojima, M., 1989. Synthesis and Evaluation of ^{11}C−PK 11195 for In Vivo Study of Peripheral-type Benzodiazepine Receptors Using Positron Emission Tomography. *Ann. Nucl. Med.* **1989**, *3*, 63−71.

(17) Cappelli, A.; Anzini, M.; Vomero, S.; De Benedetti, P. G.; Menziani, M. C.; Giorgi, G.; Manzoni, C. Mapping the Peripheral Benzodizaepine Receptor Binding Site by Conformationally Restrained Derivatives of 1-(2-Chlorophenyl)-1-*N*-methypropyl-3-isoquinolinecarboxamide (PK11195). *J. Med. Chem.* **1997**, *40*, 2910−2921.

(18) Matarrese, M.; Moresco, R. M.; Cappelli, A.; Anzini, M.; Vomero, S.; Simonelli, P.; Verza, E.; Magni, F.; Sudati, F.; Soloviev, D.; Todde, S.; Carpinelli, A.; Kienle, M. G.; Fazio, F. Labeling and Evaluation of N-[^{11}C]Methylated Quinoline-2-carboxamides as Potential Radioligands for Visualization of Peripheral Benzodiazepine Receptors. *J. Med. Chem.* **2001**, *44*, 579−585.

(19) Pike, V. W.; Halldin, C.; Crouzel, C.; Barre, L.; Nutt, D. J.; Osman, S.; Shah, F.; Turton, D. R.; Waters, S. L. Radioligands for PET Studies of Central Benzodiazepine Receptors and PK (Peripheral Benzodiazepine) Binding Sites-Current Status. *Nucl. Med. Biol.* **1993**, *20*, 503−525.

(20) Pappata, P.; Cornu, Y.; Samson, C.; Prenant, J.; Benavides, B.; Scatton, C.; Crouzel, J. J.; Hauw, A.; Syrota, A. PET Study of Carbon-11-PK11195 Binding to Peripheral Type Benzodiazepine Sites in Glioblastoma: a Case report. *J. Nucl. Med.* **1991**, *32*, 1608−1610.

(21) Cagnin, A.; Brooks, D. J.; Kennedy, A. M., Gunn, R. N.; Myers, R.; Turkheimer, F. E.; Jones, T.; Banati, R. B. In-vivo Measurement of Activated Microglia in Dementia. *Lancet* **2001**, *358*, 461−467.

(22) Banati, R. B.; Goerres, G. W.; Myers, R.; Gunn, R. N.; Turkheimer, F. E.; Kreutzberg, G. W.; Brooks, D. J., Jones, T.; Duncan, J. S. [^{11}C](R)-PK11195 Positron Emission Tomography Imaging of Activated Microglia In Vivo in Rasmussen's encephalitis. *Neurology* **1999**, *53*, 2199−2203.

(23) Debruyne, J. C.; Van Laere, K. J.; Versijpt, J.; De Vos, F.; Eng, J. K.; Strijckmans, K.; Santens, P.; Achten, E.; Slegers, G.; Korf, J.; Dierckx, R. A.; De Reuck, J. L. Semiquantification of the Peripheral-type Benzodiazepine Ligand [^{11}C]PK11195 in Normal Human Brain and Application in Multiple Sclerosis Patients. *Acta Neurol. Belg.* **2002**, *102*, 127−135.

(24) Nakazato, A.; Okubo, T.; Nakamura, T.; Chaki, S.; Tomisawa, K.; Nagamine, M.; Yamamoto, K.; Harada, K.; Yoshida, M. Aryloxyaniline derivatives. WO99/06353.

(25) Chaki, S.; Funakoshi, T.; Yoshikawa, R.; Okuyama, S.; Okubo, T.; Nakazato, A.; Nagamine, M.; Tomisawa, K. Binding Characteristics of [^{3}H]DAA1106, a Novel and Selective Ligand for Peripheral Benzodiazepine Receptors. *Eur. J. Pharmacol.* **1999**, *371*, 197−204.

(26) Okuyama, S.; Chaki, S.; Yoshikawa, R.; Ogawa, S.; Suzuki, Y.; Okubo, T.; Nakazato, A.; Nagamine, M.; Tomisawa, K. Neuropharmacological Profile of Peripheral Benzodiazepine Receptor Agonists, DAA1097 and DAA1106. *Life Sci.* **1999**, *64*, 1455−1564.

(27) Okubo, T.; Yoshikawa, R.; Chaki, S.; Okuyama, S.; Nakazato, A. Design, synthesis and structure-affinity relationships of aryloxyanilide derivatives as novel peripheral benzodiazepine receptor ligands. *Bioorg. Med. Chem.* **2004**, *12*, 423−438.

(28) Zhang, M.-R.; Kida, T.; Noguchi, J.; Furutsuka, K.; Maeda, J.; Suhara, T.; Suzuki, K.; [^{11}C]DAA1106: Radiosynthesis and In Vivo Binding to Peripheral Benzodiazepine Receptors in Mouse Brain. *Nucl. Med. Biol.* **2003**, *30*, 513−519.

(29) Maeda, J.; Suhara, T.; Zhang, M.-R.;Okauchi, T.; Yasuno, F.; Ikoma, Y.; Inaji, M.; Nagai, Y.; Ichimiya,; Ohbayashi, S.; Suzuki, K. Novel Peripheral Benzodiazepine Receptor Ligand [^{11}C]-DAA1106 for PET; An Imaging Tool for Glial Cells in the Brain. *Synapse*, in press.

(30) Zhang, M.-R.; Maeda, J.; Furutsuka, K.; Yoshida, Y.; Ogawa, M.; Suhara, T.; Suzuki, K. [^{18}F]FMDAA1106 and [^{18}F]-FEDAA1106: Two Positron-emitter Labeled Ligands for Peripheral Benzodiazepine Receptor (PBR). *Bioorg. Med. Chem. Lett.* **2003**, *13*, 201−204.

(31) Zheng, L.; Berridge, M. S. Synthesis of [^{18}F]fluoromethyl Iodide, a Synthetic precursor for Fluoromethylation of Radiopharmaceutical. *Appl. Radiat. Isot.* **2000**, *52*, 55−61.

(32) Zhang, M.-R.; Tsuchiyama, A.; Haradahira, T.; Yoshida, Y.; Furutsuka, K.;Suzuki, K. Development of an Automated System for Synthesizing ^{18}F-Labeled Compounds Using [^{18}F]Fluoroethyl Bromide as a Synthetic Precursor. *Appl. Radiat. Isot.* **2002**, *57*, 335−342.

(33) Zhang, M.-R.; Ogawa, M.; Furutsuka, K.; Yoshida, Y.; Suzuki, K. [^{18}F]Fluoromethyl Iodide ([^{18}F]FCH_2I): Preparation and Reactions with Phenol, Thiophenol, Amide and Amine Functional Groups. *J. Fluorin. Chem.*, accepted.

(34) Sihver, S.; Sihver, W.; Bergstrom, M.; Hoglund, U.; Sjoberg, P.; Langstrom, B.; Watanabe, Y. Quantitative Autoradiography with Short-lived Positron Emission Tomography Tracers: a Study on Muscarinic Acetylcholine Receptors with *N*-[^{11}C]Methyl-4-piperidylbenzilate. *J. Pharmacol. Exp. Ther.* **1999**, *290*, 917−922.

(35) Zhang, M.-R.; Haradahira, T.; Maeda, J.; Okauchi, T.; Kawabe, K.; Kida, T.; Obayashi, S.; Suzuki K.; Suhara T. Synthesis and Evaluation of 3-(4-Chlorobenzyl)-8-[^{11}C]methoxy-1,2,3,4-tetrahydrochromeno[3,4-*c*]pyridin-5-one: a PET Tracer for Imaging $Sigma_1$ Receptors. *Nucl. Med. Biol.* **2002**, *29*, 469−476.

(36) Petit-Taboué, M. C.; Baron, J. C.; Barré, L.; Travère, J. M.; Speckel, D.; Camsonne, R.; MacKenzie, E. T. Brain Kinetics and Specific Binding of [^{11}C]PK 11195 to Omaga3 Sites in Baboons: Positron Emission Tomography Study. *Eur. J. Pharmacol.* **1991**, *200*, 347−351.

(37) Cheng, Y. C.; Prusoff, W. H. Relationship between Inhibition Constant (Ki) and the Concentration of Inhibitor Which Causes 50 Percent Inhibition (IC50) of an Enzymatic Reaction. *Biochem. Pharmacol.* **1973**, *92*, 881−894.

(38) Maeda, J.; Suhara, T.; Kawabe, K.; Okauchi, T.; Obashi S.; Hojo J.; Suzuki K. Visualization of α5 Subunit of $GABA_A$/Benzodiazepine Receptor by [^{11}C]Ro15−4513 Using Positron Emission Tomography. *Synapse.* **2003**, *47*, 200−208.

JM0304919